AD

AD-E401 980

Contractor Report ARCCD-CR-89005

FINITE ELEMENT ANALYSIS OF 30-mm CARTRIDGE CASE

Michael Giltrude
Advanced Technology and Research, Inc
14900 Sweitzer Lane, Suite 104
Laurel, MD 20707

Linda Havron
Project Engineer
ARDEC

DTIC
ELECTE
NOV.15.1989
S B D

October 1989

U.S. ARMY ARMAMENT RESEARCH, DEVELOPMENT AND ENGINEERING CENTER

Close Combat Armaments Center

Picatinny Arsenal, New Jersey

US ARMY
ARMAMENT MUNITIONS
& CHEMICAL COMMAND
ARMAMENT RDE CENTER

AD-A214 396

89 11 13 109

The views, opinions, and/or findings contained in this report are those of the author(s) and should not be construed as an official Department of the Army position. policy. or decision, unless so designated by other documentation.

The citation in this report of the names of commercial firms or commercially available products or services does not constitute official endorsement by or approval of the U.S. Government.

Destroy this report when no longer needed by any method that will prevent disclosure of contents or reconstruction of the document. Do not return to the originator.

REPORT DOCUMENTATION PAGE

1a. REPORT SECURITY CLASSIFICATION UNCLASSIFIED	1b. RESTRICTIVE MARKINGS
2a. SECURITY CLASSIFICATION AUTHORITY	3. DISTRIBUTION/AVAILABILITY OF REPORT Approved for public release; distribution is unlimited.
2b. DECLASSIFICATION/DOWNGRADING SCHEDULE	

4. PERFORMING ORGANIZATION REPORT NUMBER	5. MONITORING ORGANIZATION REPORT NUMBER Contractor Report ARCCD-CR-89005

6a. NAME OF PERFORMING ORGANIZATION Advanced Technology and Research, Inc.	6b. OFFICE SYMBOL	7a. NAME OF MONITORING ORGANIZATION ARDEC, CCAC
6c. ADDRESS (CITY, STATE, AND ZIP CODE) 14900 Sweitzer Lane, Suite 104 Laurel, MD 20707		7b. ADDRESS (CITY, STATE, AND ZIP CODE) Light Armament Division (SMCAR-CCL-CH) Picatinny Arsenal, NJ 07806-5000
8a. NAME OF FUNDING/SPONSORING ORGANIZATION ARDEC, IMD STINFO Br	8b. OFFICE SYMBOL SMCAR-IMI-I	9. PROCUREMENT INSTRUMENT IDENTIFICATION NUMBER

8c. ADDRESS (CITY, STATE, AND ZIP CODE) Picatinny Arsenal, NJ 07806-5000	10. SOURCE OF FUNDING NUMBERS			
	PROGRAM ELEMENT NO.	PROJECT NO.	TASK NO.	WORK UNIT ACCESSION NO.

11. TITLE (INCLUDE SECURITY CLASSIFICATION)

FINITE ELEMENT ANALYSIS OF 30-mm CARTRIDGE CASE

12. PERSONAL AUTHOR(S) Michael Giltrude, Advanced Technology Research, Inc. and Linda Havron, Proj Engr, ARDEC

13a. TYPE OF REPORT Final	13b. TIME COVERED FROM _____ TO _____	14. DATE OF REPORT (YEAR, MONTH, DAY) October 1989	15. PAGE COUNT 46

16. SUPPLEMENTARY NOTATION

17. COSATI CODES			18. SUBJECT TERMS (CONTINUE ON REVERSE IF NECESSARY AND IDENTIFY BY BLOCK NUMBER)
FIELD	GROUP	SUB-GROUP	Finite element analysis/ Stress-strain curve /
			Case-bolt interaction modeling) Case-barrel interaction modeling / (

19. ABSTRACT (CONTINUE ON REVERSE IF NECESSARY AND IDENTIFY BY BLOCK NUMBER)

During ballistic testing, the 30-mm cartridge case has occasionally coined in the barrel of the M230 gun under unidentifiable conditions. An elastic-plastic stress analysis with increasing ballistic pressure loading up to 70 ksi for the friction and frictionless cases of the 30-mm thin wall steel cartridge case mounted in the M230 gun was performed using the ANSYS finite element computer code. These analyses were carried out to evaluate the response of the cartridge case-barrel-bolt assembly due to the effects of pressure loads. Based on the results obtained, it was found that at the maximum applied pressure (70 ksi) no coining developed in the cartridge case-bolt contact zone.

20. DISTRIBUTION/AVAILABILITY OF ABSTRACT ☐ UNCLASSIFIED/UNLIMITED ☒ SAME AS RPT. ☐ DTIC USERS	21. ABSTRACT SECURITY CLASSIFICATION UNCLASSIFIED	
22a. NAME OF RESPONSIBLE INDIVIDUAL I. HAZNEDARI	22b. TELEPHONE (INCLUDE AREA CODE) (201) 724-3316	22c. OFFICE SYMBOL SMCAR-IMI-I

DD FORM 1473, 84 MAR

CONTENTS

FIGURES

FIGURES (cont)

INTRODUCTION

During ballistic testing, the 30-mm cartridge case occasionally coined in the barrel of the M230 gun under unidentifiable conditions. The coining results from the plastic deformation of the case expanding into the barrel due to ballistic loads. This can result in the jamming of the gun. The coining effect may also be accentuated by setback forces. These forces are caused when a lubricated round fails to obturate properly.

Establishing the relative position between the case and chamber at the instant of firing is important because it determines the radial gap between the case and the barrel chamber. As the propellant gases are generated, the case expands until the gap is closed. When the case comes in contact with the chamber, any remaining buildup in pressure is transferred to the heavy wall of the barrel, which deflects only a small additional amount. Therefore, the barrel restrains the case which limits the peak hoop stress in the thin-wall portion of the cartridge case. A schematic view of the bolt assembly is shown in figures 1 and 2.

ANALYTICAL METHOD

An elastic-plastic stress analysis with increasing ballistic pressure loading up to 70 ksi for the friction and frictionless cases of the 30 mm thin wall steel cartridge case mounted in the M230 gun was performed using the ANSYS finite element computer code (ref 1).

The ANSYS code uses the finite element displacement method to determine the response of arbitrarily shaped structures to arbitrary loading. For this analysis, the ANSYS preprocessor, PREP7 is used to create an axisymmetric finite element model using four noded quadrilateral elements and two noded gap elements. The response of the model to a nonlinear static analysis at various internal pressure loadings up to 70 ksi was investigated. Sources of nonlinearities include the use the gap elements and plasticity associated with the cartridge case material. Results in the form of plots of iso-stress lines and displacements as well as tabulations of element stresses are presented using the ANSYS supplied postprocessor POST 1.

MATERIALS MODELS

The barrel and bolt are assumed to have elastic material properties (fig. 3). The cartridge case (10B22 steel) is modeled using the classical bilinear kinematic hardening option provided by the ANSYS code. This option assumes that the total stress range is equal to twice the yield stress so that the Bauschinger effect is included. Based on

results from previous studies (ref 2), the strain rate was assumed to be a constant 400 in./in./s, a value which is representative of these types of problems. At this strain rate, the allowable strain energy to failure increases by 7% with respect to that of the static case. The properties for 10B22 steel are shown in figure 4.

ANALYSIS OF THE CARTRIDGE CASE

Finite Element Model

The thin walled steel cartridge and barrel were modeled using the nominal dimensions shown in figure 5. A portion of the bolt (fig. 6) was also included to obtain reaction forces. The breech (figs. 7 and 8) was not included in the model since its effect on the cartridge case was assumed to be insignificant.

Axisymmetric elements were chosen to take advantage of the symmetry of the system and reduce computer run time. Surface stress printout was selected for the elements located at the cartridge/barrel interface. The interface was modeled using 24 gap elements. The gaps, when closed, were investigated with and without frictional effects. A schematic of the model is shown in figure 9.

Boundary Conditions

The nominal boundary conditions imposed on the model are shown in figure 9. The bolt is restrained in the axial direction to provide a base against which the cartridge can react. The barrel is also restrained in the axial direction to prevent it from drifting away before the gap closes. The pressure is applied normal to the inside surface of the cartridge. The initial magnitude of 3000 psi was calculated to initiate plastic deformation. Subsequent restarts incremented the pressure up to 70 ksi. A dimensional analysis using nominal values indicated an open gap in the unloaded condition. The condition of the gaps under subsequent loads was determined by the program. The partial support provided by the two-bolt grips holding the cartridge case head was not included in the analysis. It was concluded by engineering judgment that by not including the bolt grips, the model would remain axisymmetrical and yet provide conservative results.

Case-Bolt Interaction Modelling

The irregular shape of the bolt surface impacting against the case head is shown in figure 6. The bolt head is shaped like an irregular gear with seven teeth. The case head diameter in contact with the bolt is smaller than the bolt outer diameter but greater than the bolt base diameter.

In order to investigate the possibility of coining in the cartridge case when setback forces are transmitted from the bolt, two sets of boundary conditions were used. The first boundary condition set provided full support throughout the entire case head. Therefore, the effective bolt diameter was assumed to be equal to the case head diameter. The second boundary condition provided only partial bolt support at the contact area. As a result, the bolt contact area was limited to that covered by the bolt base diameter (16 mm). This last assumption represented an extreme condition devised only to obtain upper stress bounds at the case-bolt interface. The effect of the irregularly shaped bolt is simulated without violating axial symmetry.

Case-Barrel Interaction Modeling

Nominal cartridge and barrel dimensions from figure 5 was used to establish the initial gap between these components. Gap elements were used to monitor the status of the interface. An amplified view of these gap elements is shown in figure 10. As the pressure builds, the cartridge expands to close the gap and push against the bolt. At this point, any further buildup of pressure is transferred to the barrel and limits the peak hoop stress in the cartridge. Two conditions are considered when the gap closes, friction and no friction.

The effects of friction are to oppose the pressure pushing the cartridge against the bolt. This should minimize the amount of coining that occurs. A coefficient of friction of 0.3 was selected per reference 3 for the nominal case. This value was changed to zero to represent the situation of a lubricated round in the breech.

Summary of Computer Solutions

Stress contour plots (figs. 11 to 32) summarize the three sets of computer solutions obtained.

Three separate analyses were conducted on the barrel-case-bolt assembly. The first analysis, the nominal case, included the effects of frictional forces between the case and the barrel. The second one, representing the lubricated round condition (nonfrictional case), did not include frictional effects. Full contact area between the case head and the bolt was assumed in these two analyses. The third analysis was developed to study the extreme coining effects existing when the area of contact between the case head and the bolt is minimum and no frictional forces occur between the case and barrel.

Frictional Case, Nominal Conditions

A friction coefficient of 0.30 (obtained from studies described in ref 3) was used for the first analysis which started with an initial internal pressure of 3 ksi. The pressure load was then gradually incremented from 3 to 70 ksi.

At the initial pressure level of 3.0 psi, all gaps remained open. It was observed from the nodal stress contour plot (fig. 11) that peak nodal equivalent stresses reached 170 ksi at the right end of the case neck area. Stresses across the thin case wall ranged from 30 to 90 ksi.

At 5 ksi of pressure, gaps located in the case neck area began to close (fig. 12). Equivalent stresses within the neck zone reached yield levels (>153 ksi). Stresses across the middle section of the thin case wall ranged between 30 and 110 ksi. As the first gaps began to close, hoop stresses initiated within the barrel. At 5 ksi of internal pressure, peak nodal stresses in the barrel were less than 3 ksi.

As pressure was increased, remaining gaps continued to close. A stress wave propagation spreading from the neck region towards the case belt zone was observed. A plastic region developed between the neck and the far right end of the case when the applies pressure reached 7 ksi (fig. 14).

At 20 ksi of pressure, 85% of the specified gaps were found to be closed (fig. 16). The other 15%, corresponding to the four gaps located near the case belt, remained opened throughout the entire load history. Stresses in the barrel varied from 10 ksi in the outer surface up to 35 ksi in the inner surface.

At 30 ksi of pressure, the entire case thin wall had yielded and remained in contact with the barrel (fig. 17).

At 40 ksi of pressure, stresses at the convex surface of the case head reached the yield level. However, equivalent stresses at the contact area between the case and bolt were less than 30 ksi (fig. 18). Equivalent strains throughout 90% of the case volume were below the elastic limit (0.51%). Strains in the case neck region reached up to 2.7%, which is greater than the strain yield limit.

At the final pressure value of 70 ksi, peak equivalent stresses along the case-bolt contact area were less than 50 ksi, well below the yield level of the case material (153 ksi). A few stress concentrations were observed in the cartridge case. These included the convex surface of the case head, the external case belt surface, and the internal edges of the case head. Maximum stresses at these concentrations were in excess of 140 ksi (fig. 19). Total strains in the convex case surface were 0.77%, while strains in the far case neck end were 2.9%.

Nonfrictional Case, Lubricated Round

Results from the nonfrictional case analysis are shown in figures 21 through 31. It is observed from these equivalent stress plots that the stress distributions and stress levels at the barrel and thin-wall case areas are similar to those obtained in the frictional case runs. However, stress levels at the cartridge case head section changed. At 40 ksi of pressure, the formation of stress concentrations of up to 150 ksi at the circumferential channel adjacent the the belt of the case head were observed, compared to 80 ksi found in the same zones of the frictional case. At the peak pressure of 70 ksi, stress variations throughout the entire assembly were essentially equivalent to those obtained in the frictional case. Total strains along the bolt-case surface were below the elastic limits. The maximum strains in the thin-wall section and far neck areas were 0.8% and 3.0%, respectively.

Minimum Case-Bolt Contact Area Analysis

In order to assess the effects of coining in the case head due to the partial reaction support provided by the bolt, a few bolt elements were removed from the model. As a result, the effective bolt area was given a reduced diameter of 16 mm. Because of the conservative boundary conditions imposed on this model, the results obtained from this alysis represent upper bound values.

Results corresponding to 50 and 70 ksi of applied pressure are shown in figures 31 and 32. At 70 ksi of pressure, equivalent stresses throughout the barrel and thin-wall regions of the case were found to be comparable to those obtained from the frictional case run (fig. 32). However, the state of stresses in the head region of the cartridge case had a different distribution fro those of the first two analyses. Stress and strain levels across the case surface in contact with the bolt were below 150 ksi and 0.51%, respectively. These levels are within the elastic limit. A sharp stress concentration of 220 ksi was found along the case-bolt surface. This stress concentration is artificial and should be ignored since the actual boundary conditions provide far greater restraint to the case head, impeding the formation of such types of stress concentration.

The results obtained from this last run confirm that no coining effect takes place along the cartridge case surface in contact with the bolt, since the average equivalent stresses obtained for the worst case boundary condition are less than the yield level (153 ksi) of the case material. This means that any deformation in the cartridge case head zone will vanish once the maximum ballistic pressure is released, thus impeding any coining of the case material.

CONCLUSIONS

Structural response analyses were performed on the 30 mm thin wall steel cartridge case and barrel of the M230 gun. These analyses were carried out to evaluate the response of the cartridge case-barrel-bolt assembly due to the effects of pressure loads. These analyses were performed using the ANSYS finite element code. Nonlinearities due to elastroplastic material properties and frictional gap interference fits (between case wall and barrel) were included. Regions where stress concentrations and plastic zones were developed were identified by these analyses. Based on the results obtained, it was found that at the maximum applies pressure (70 ksi) no coining develops in the cartridge case-bolt contact zone.
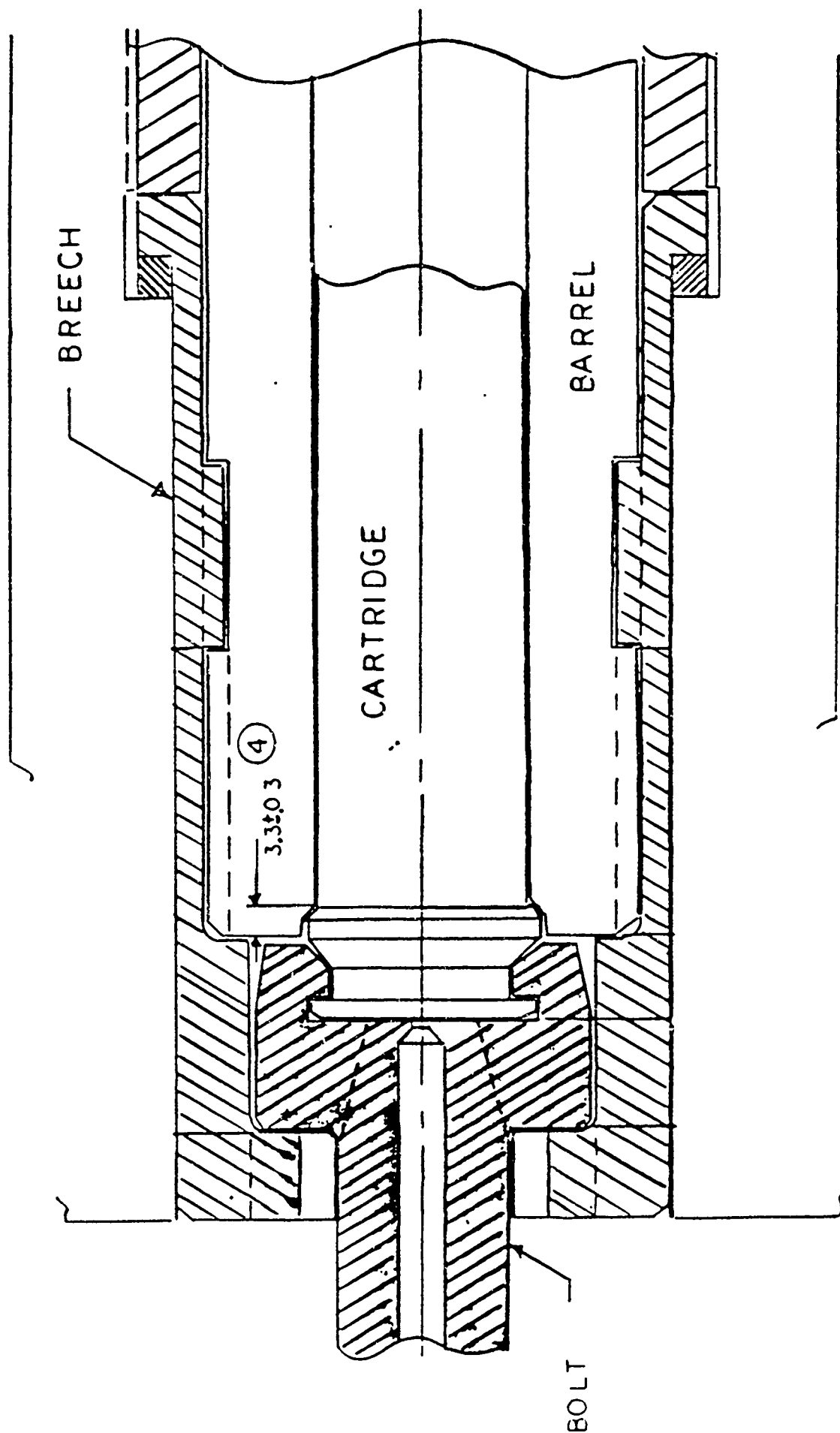
Figure 1. 30 mm cartridge case assembly

30 mm CARTRIDGE CASE
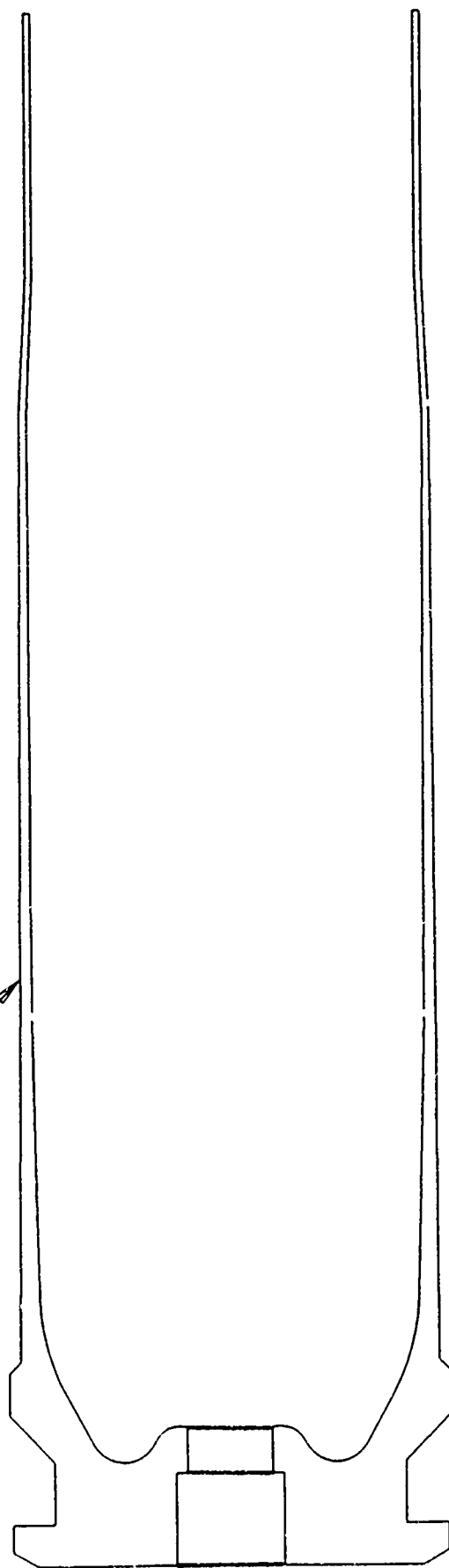
Figure 2. Cartridge case cross section
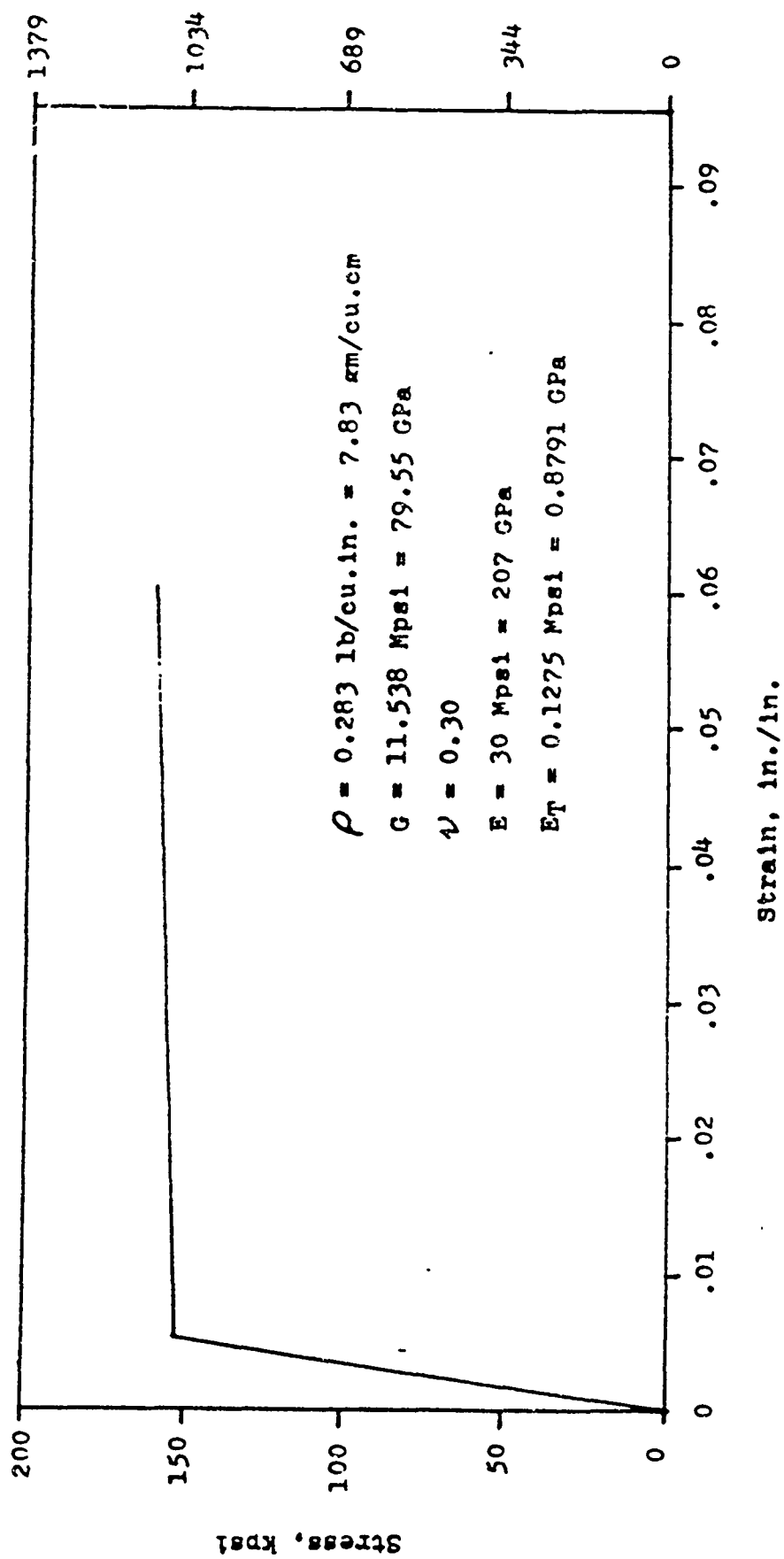
Figure 3. 10B22 steel stress-strain curve

$\rho = 0.283$ lb/cu.in. = 7.83 gm/cu.cm

$G = 11.538$ Mpsi = 79.55 GPa

$\nu = 0.30$

$E = 30$ Mpsi = 207 GPa

$E_T = 0.1275$ Mpsi = 0.8791 GPa

Stress, MPa

1724 1379 1034 689 344 0

ρ = 0.283 lb/in^3 = 7.83 gm/cm^3

G = 11 x 10^6 psi = 75.8 GPa

ν = 0.318

E = 29 Mpsi = 200 GPa

E_T = 0.2932 Mpsi = 2.022 GPa

.12 .10 .08 .06 .04 .02 0.0

Strain, in./in.

Stress, kpsi

250 200 150 100 50 0
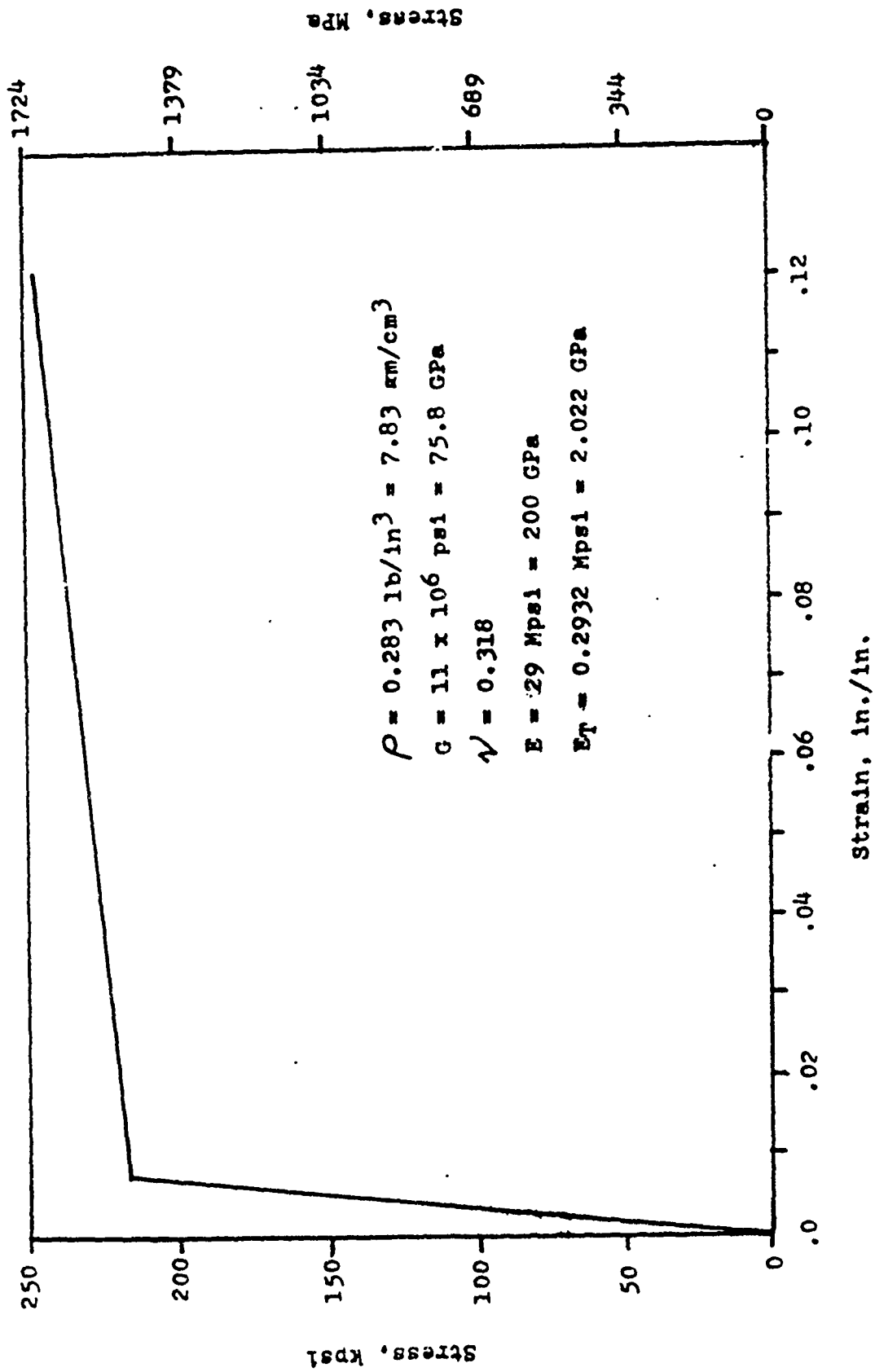
Figure 4. 4340 steel stress-strain curve

10
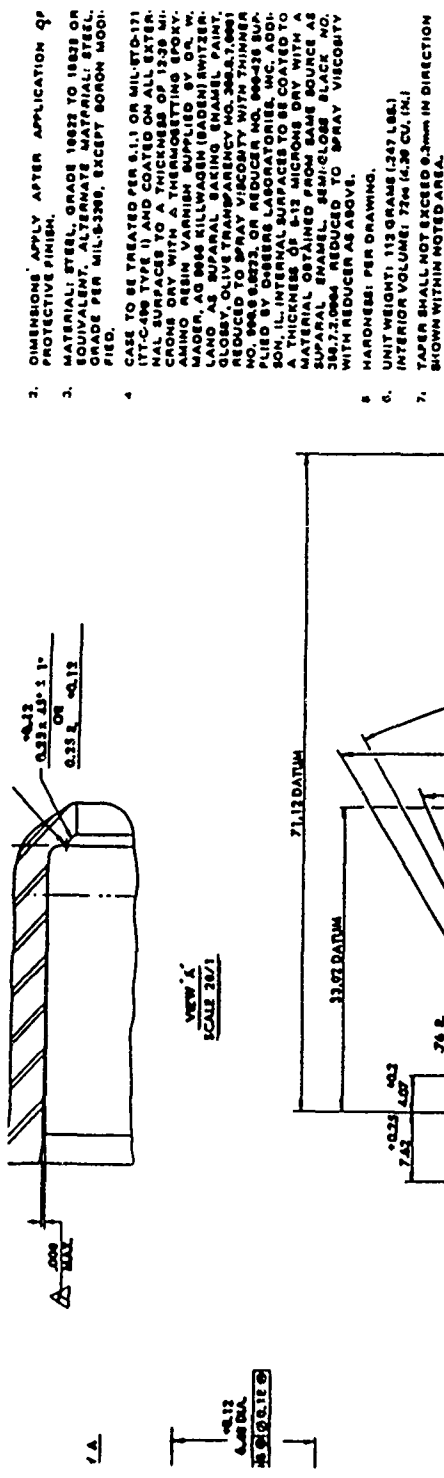
Figure 5. 30 mm steel cartridge case

11

Figure 6. Bolt detail

12

Figure 7. Breech, side view

13
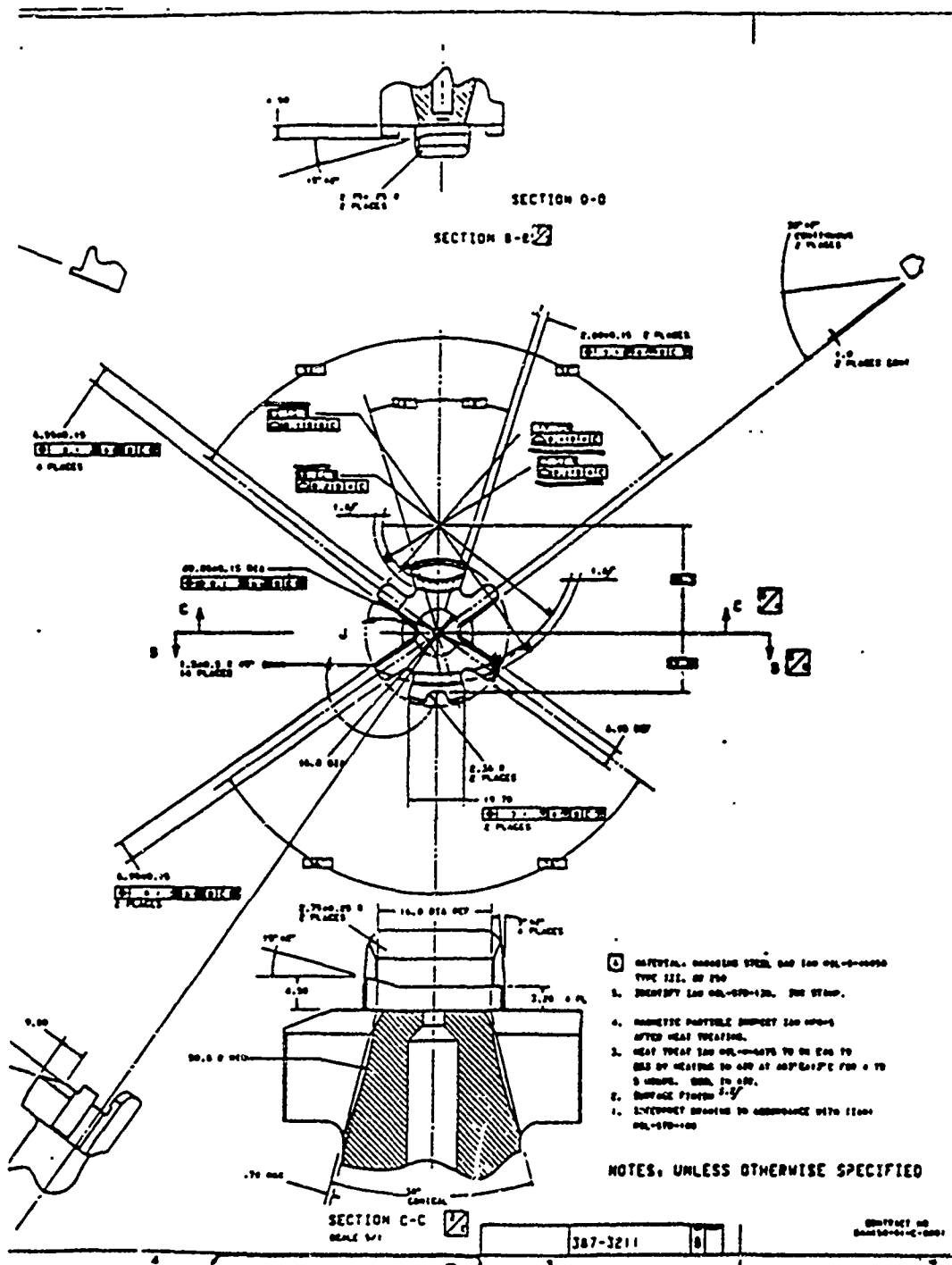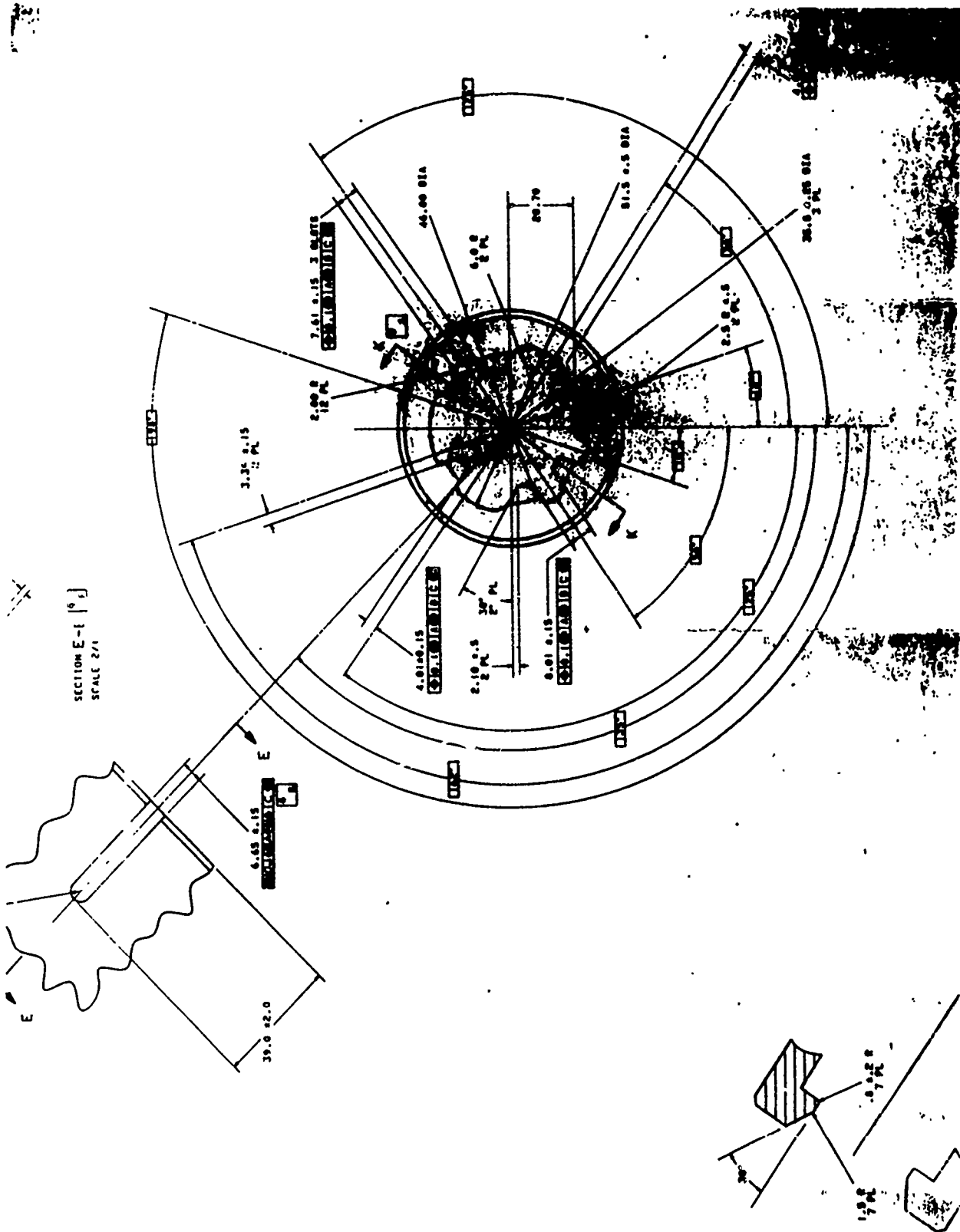
Figure 8. Breech detail, front

14
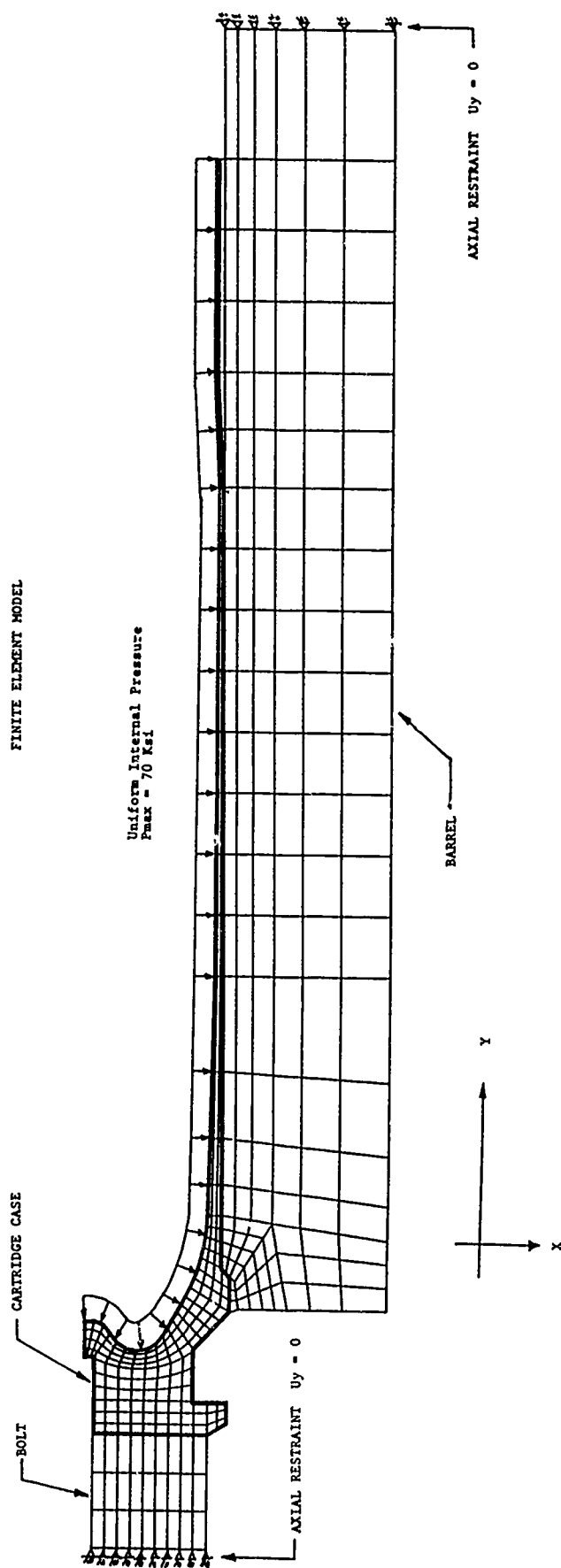
Figure 9. 30 mm steel cartridge case, finite element model
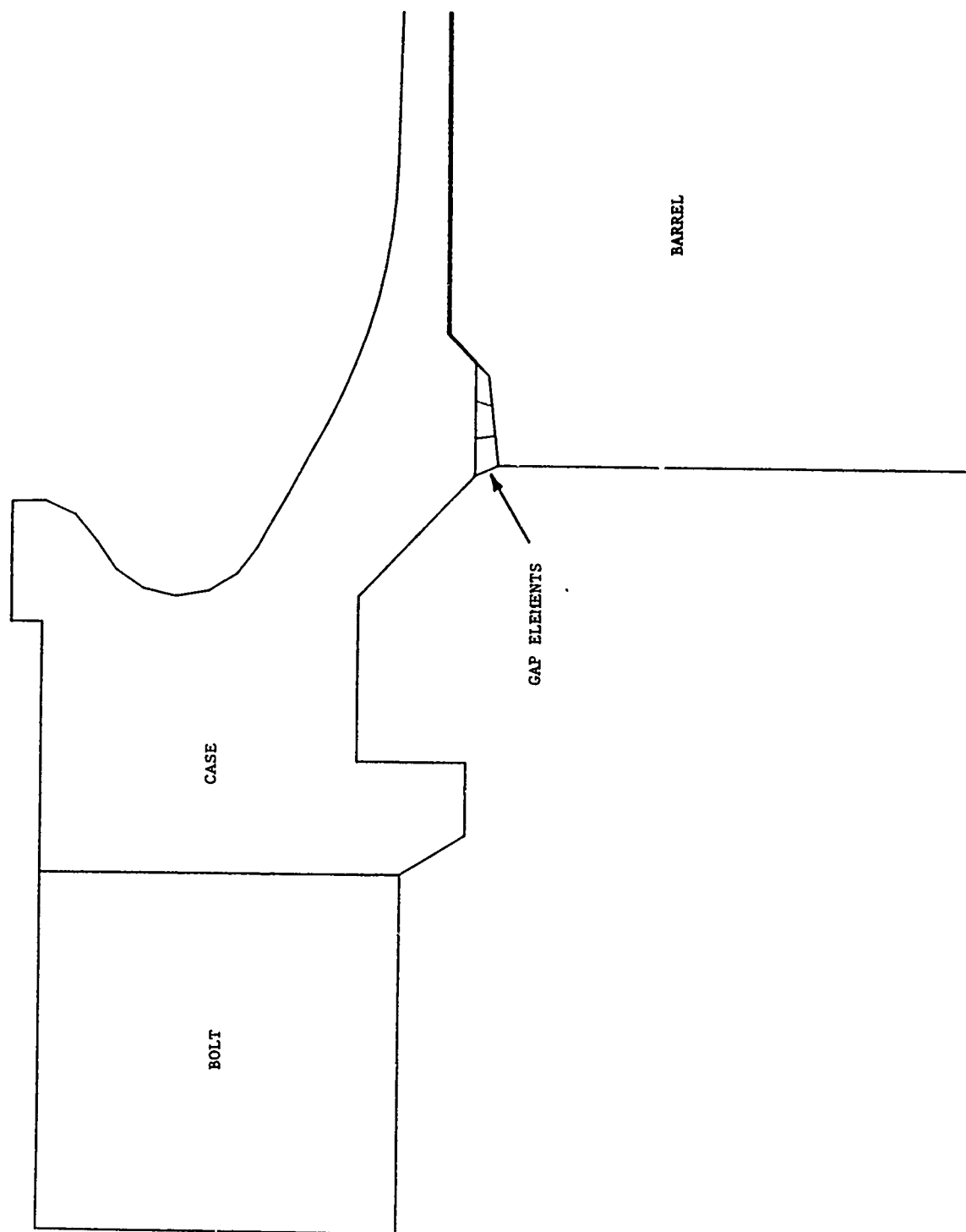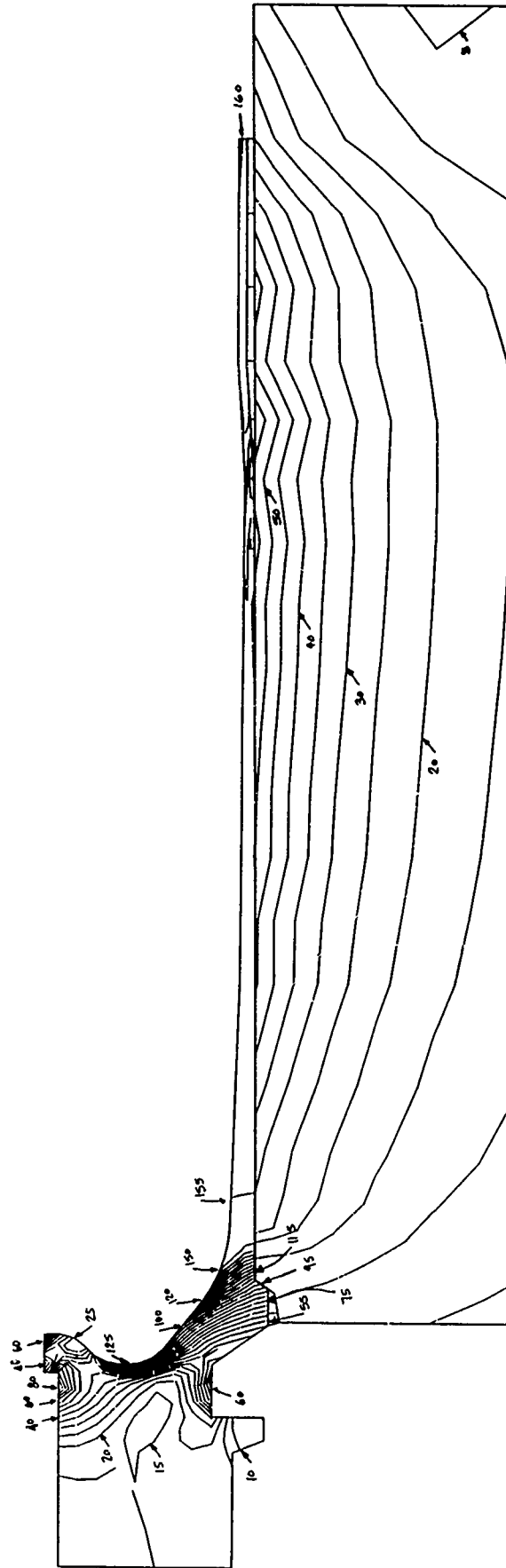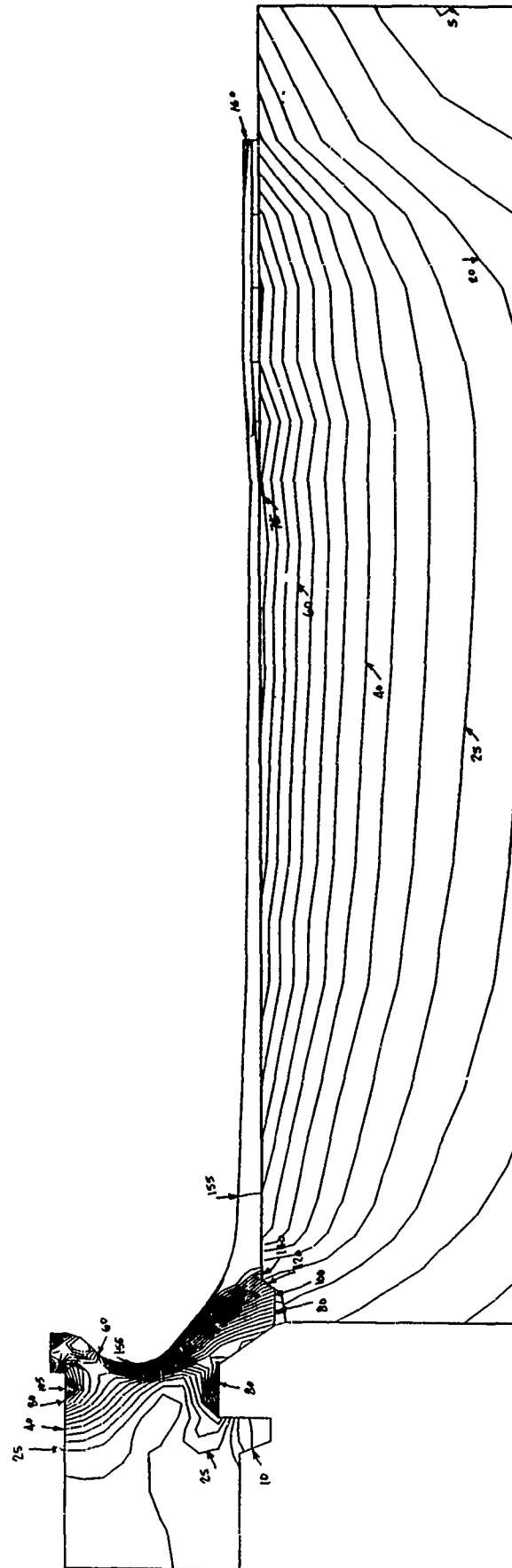
Figure 10. 30 mm steel cartridge case, gap element
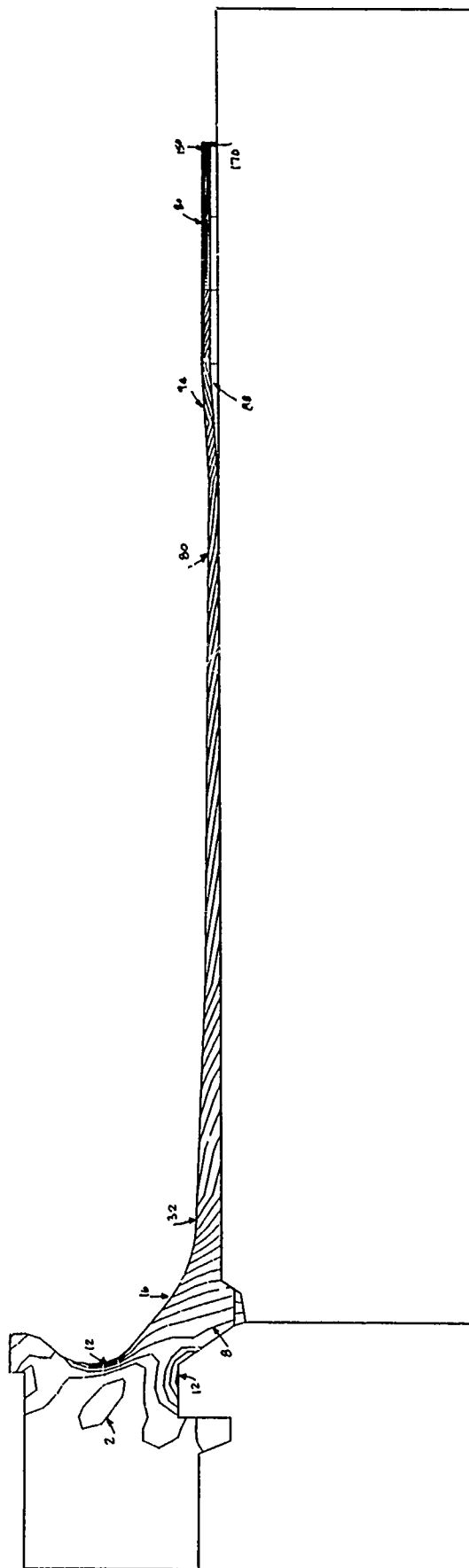
Figure 11. Equivalent stress contours, frictional case, applied pressure = 3 ksi
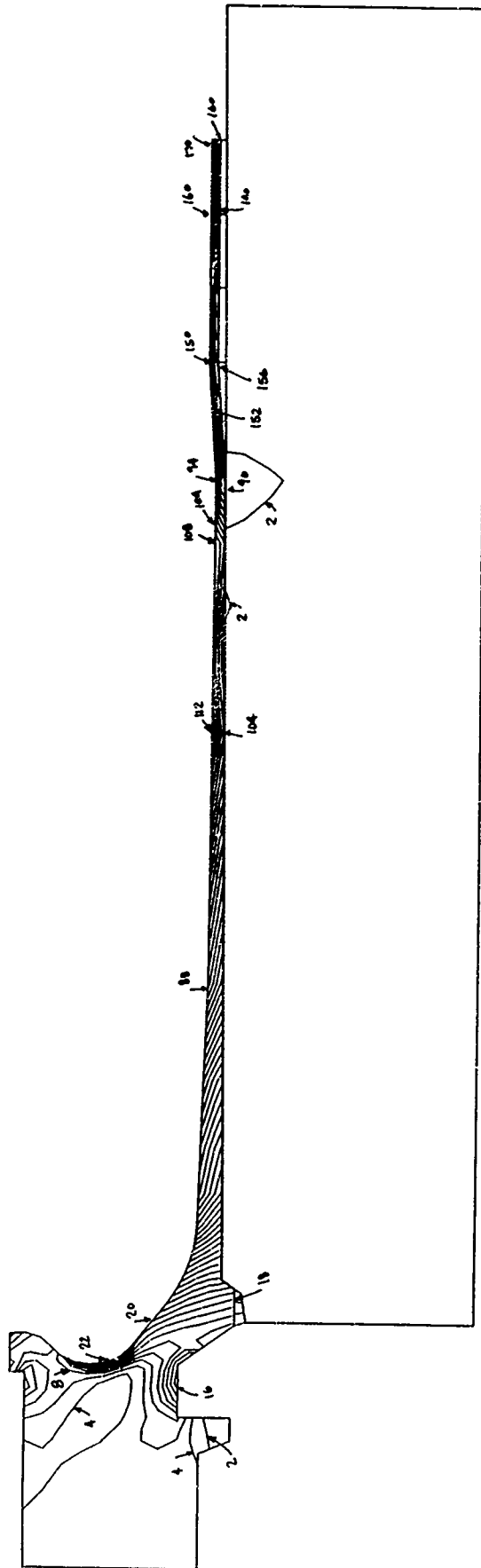
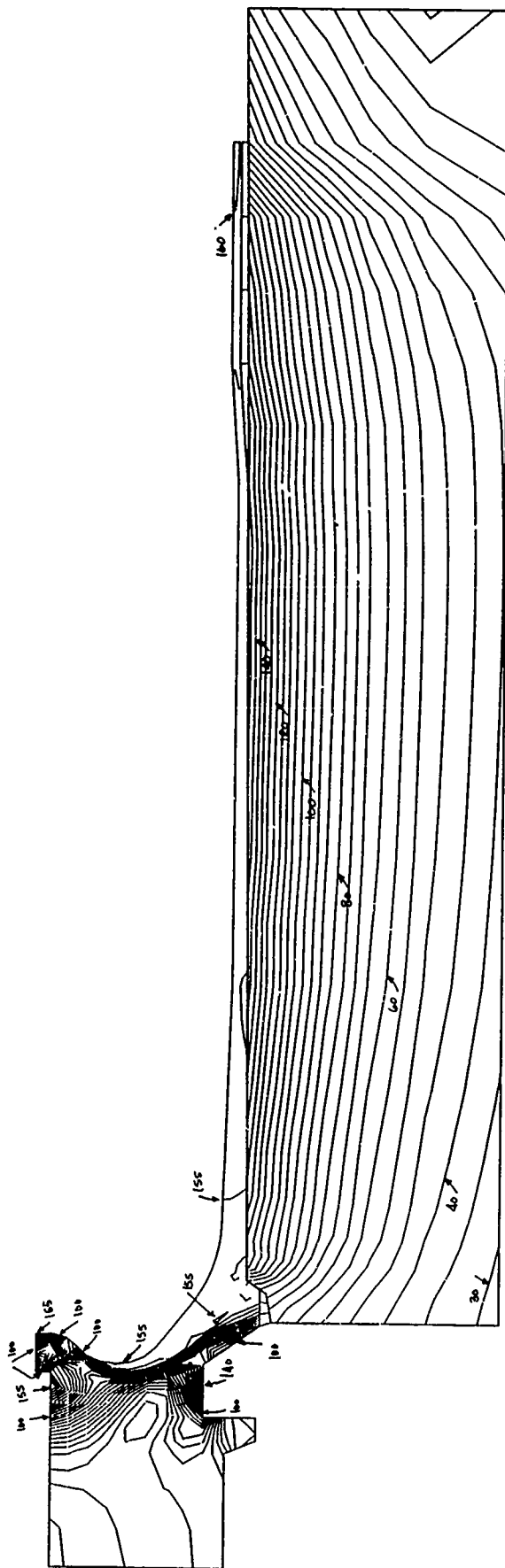Figure 12. Equivalent stress contours, frictional case, applied pressure = 5 ksi
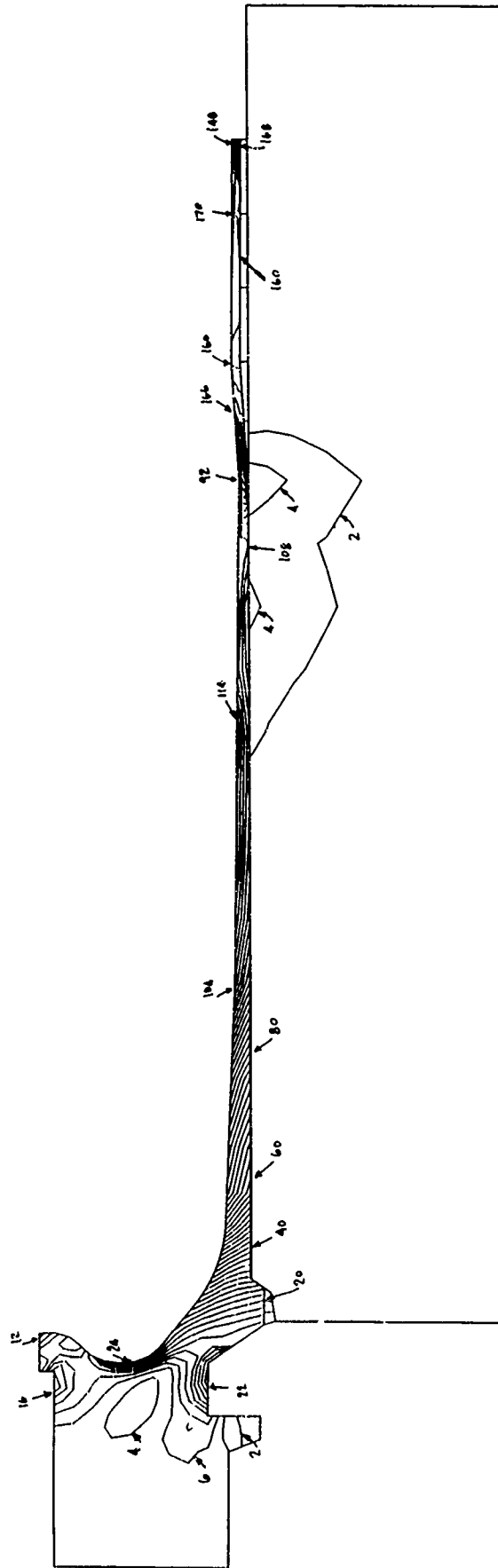
Figure 13. Equivalent stress contours, frictional case, applied pressure = 6 ksi
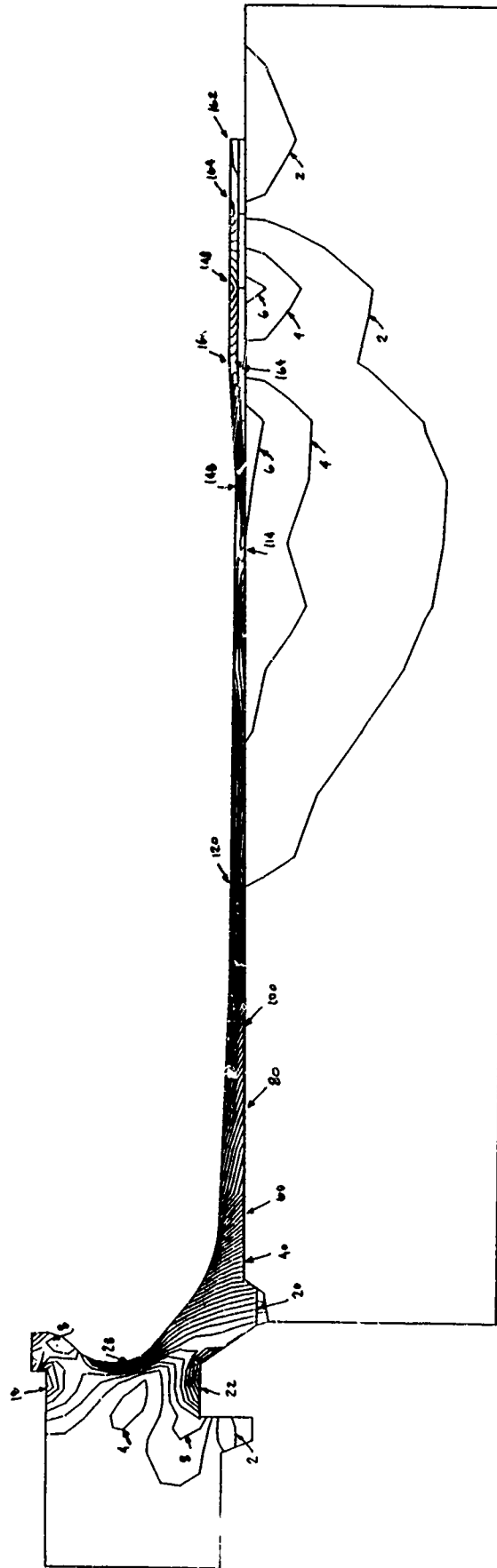
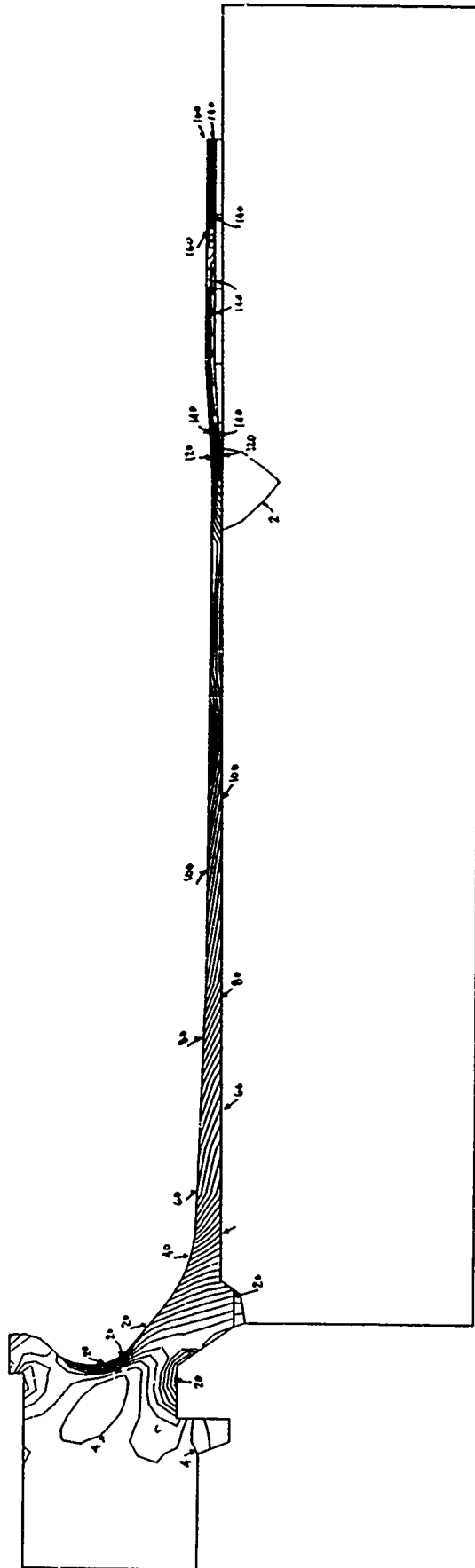Figure 14. Equivalent stress contours, frictional case, applied pressure = 7 ksi
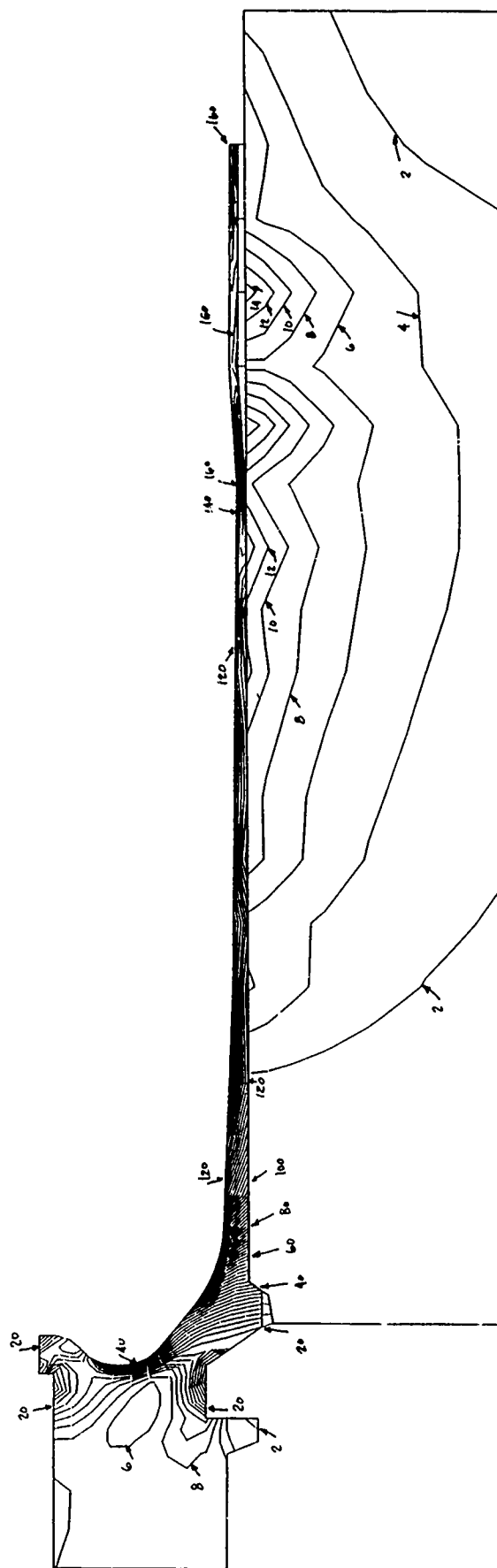
Figure 15. Equivalent stress contours, frictional case, applied pressure = 10 ksi
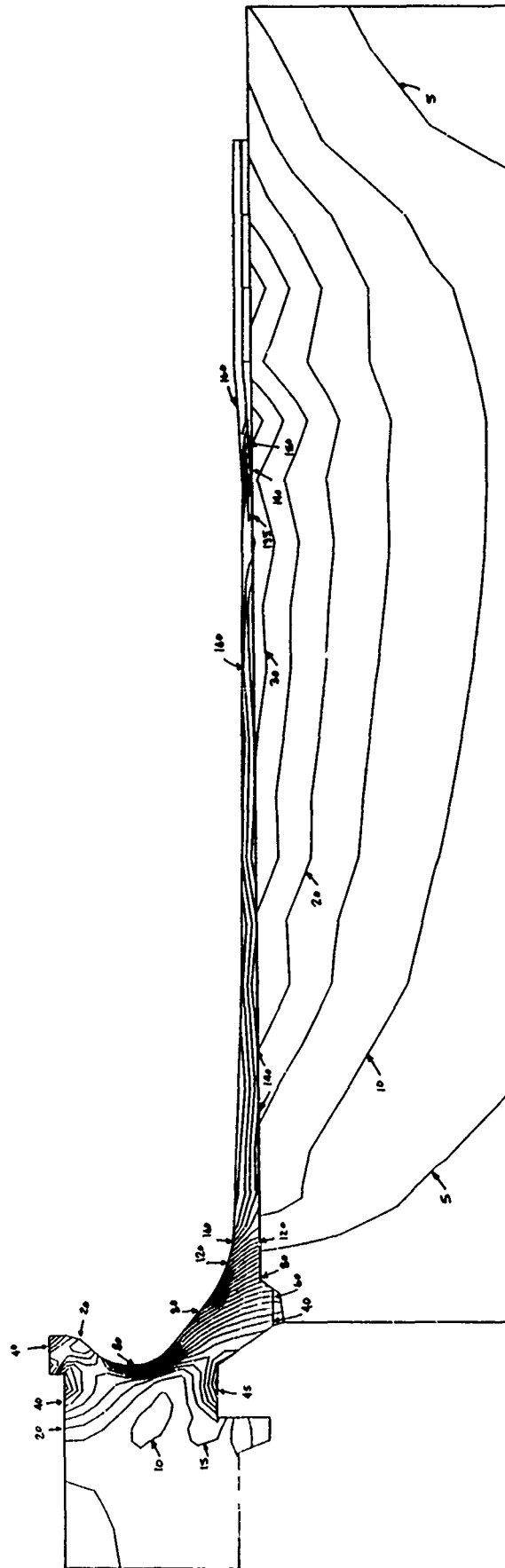
Figure 16. Equivalent stress contours, frictional case, applied pressure - 20 ksi

Figure 17. Equivalent stress contours, frictional case, applied pressure = 30 ksi

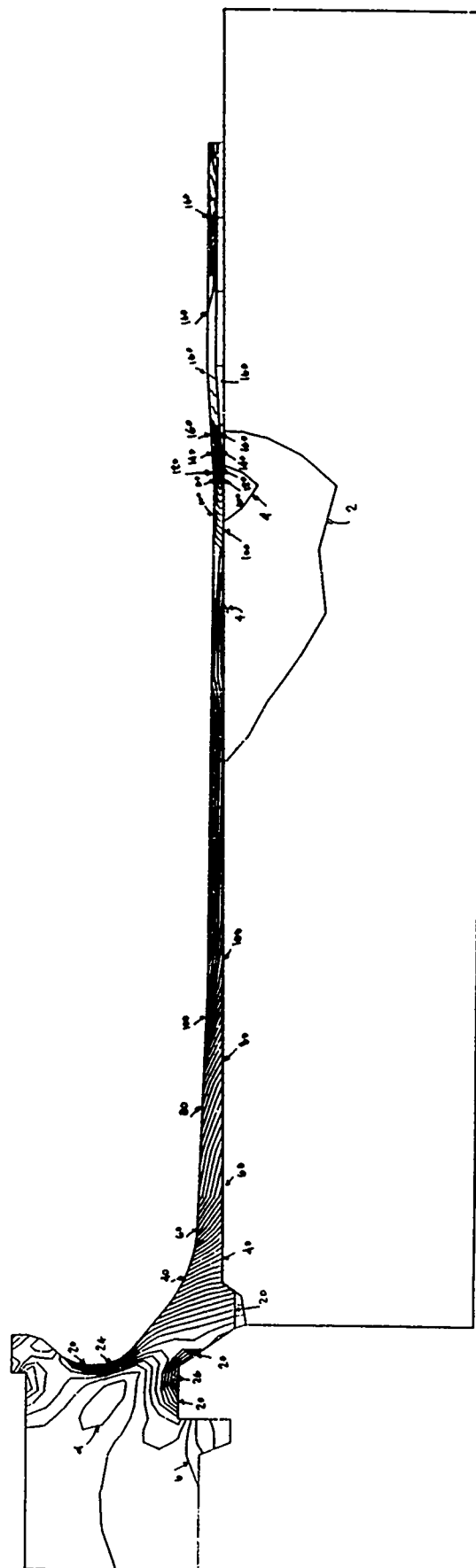Figure 18. Equivalent stress contours, frictional case, applied pressure = 40 ksi

Figure 19. Equivalent stress contours, frictional case, applied pressure = 70 ksi

Figure 20. Equivalent stress contours, nonfrictional case, applied pressure = 3 ksi

Figure 21. Equivalent stress contours, nonfrictional case, applied pressure = 5 ksi
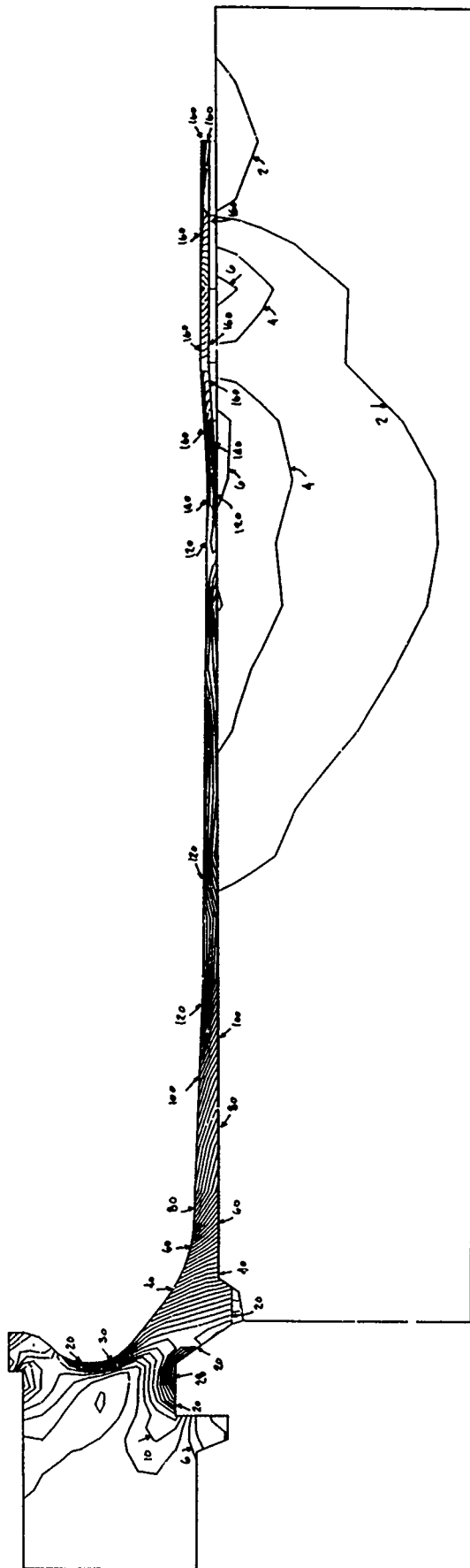
Figure 22. Equivalent stress contours, nonfrictional case, applied pressure = 6 ksi

Figure 23. Equivalent stress contours, nonfrictional case, applied pressure = 7 ksi
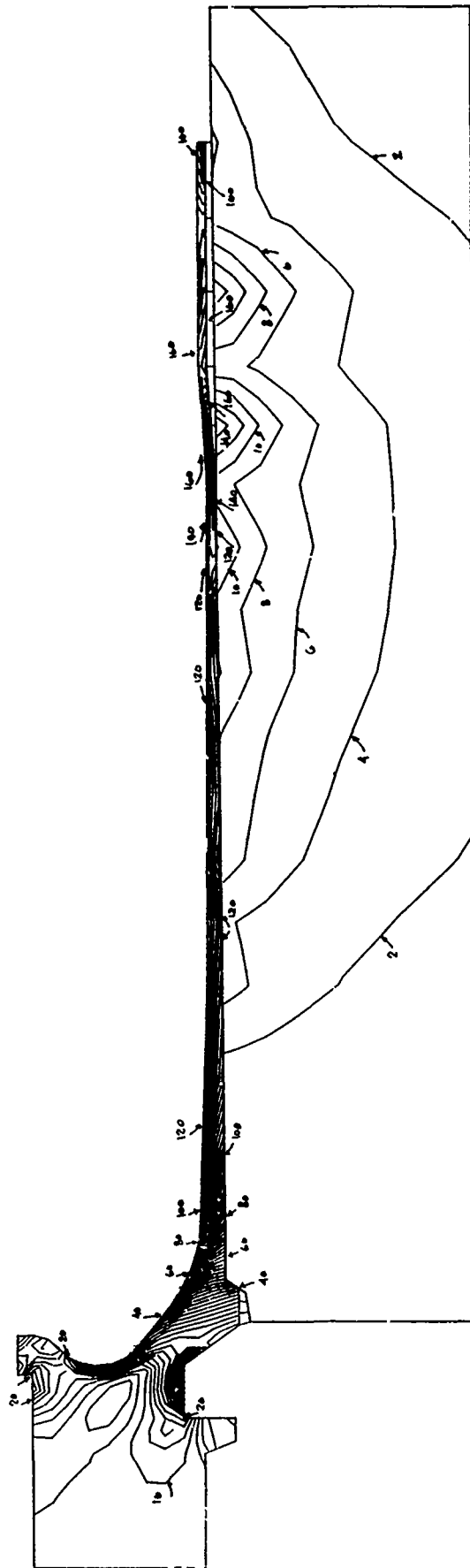
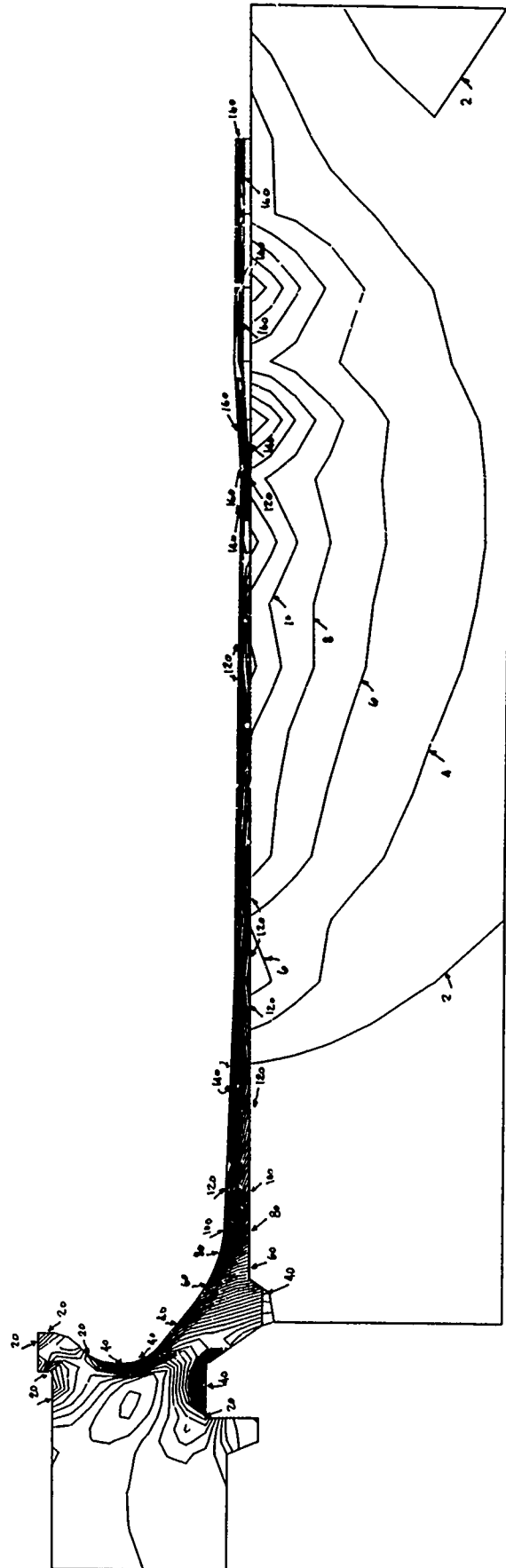Figure 24. Equivalent stress contours, nonfrictional case; applied pressure = 9 ksi

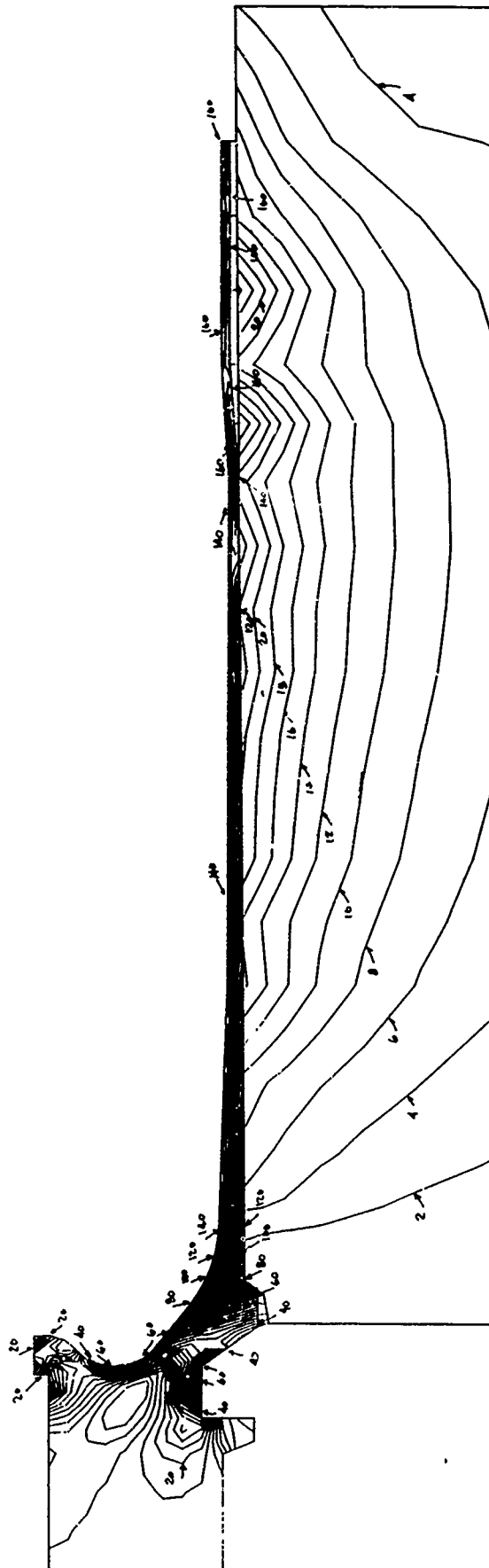Figure 25. Equivalent stress contours, nonfrictional case, applied pressure = 10 ksi

Figure 26. Equivalent stress contours, nonfrictional case, applied pressure = 15 ksi
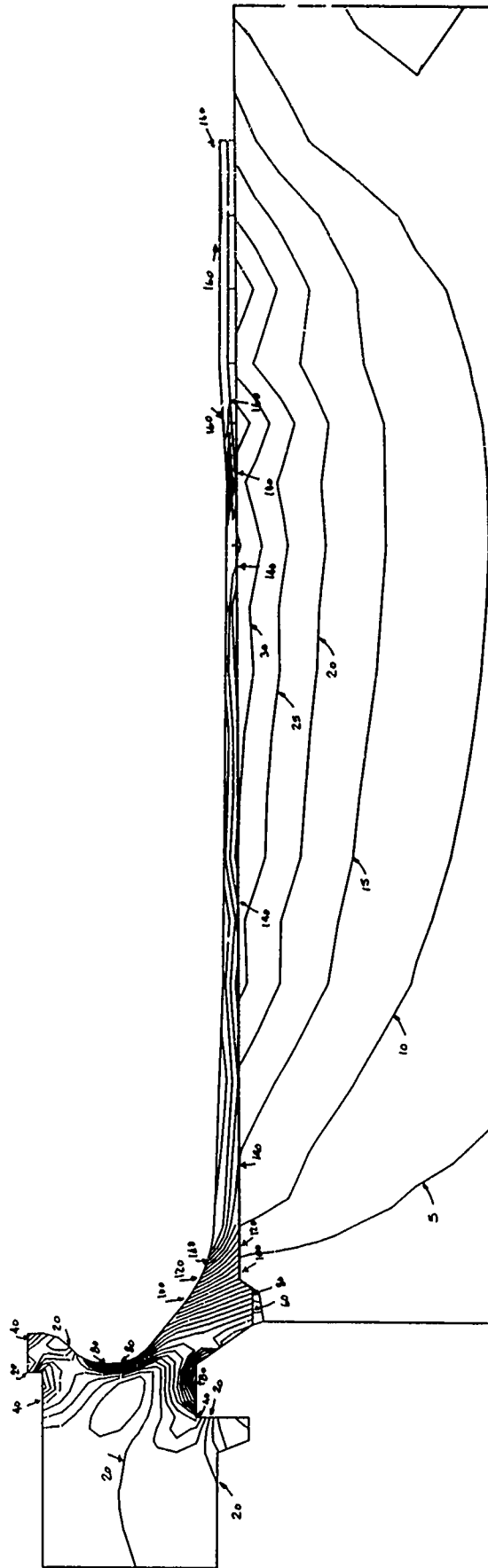
Figure 27. Equivalent stress contours, nonfrictional case, applied pressure = 20 ksi
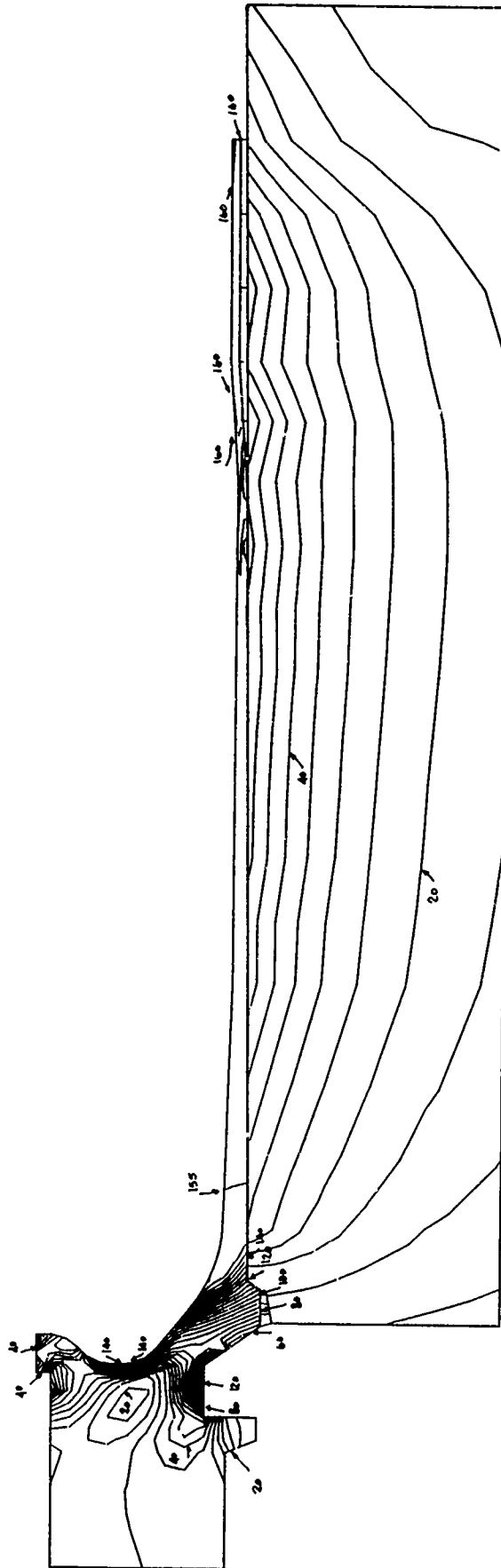
Figure 28. Equivalent stress contours, nonfrictional case, applied pressure = 30 ksi
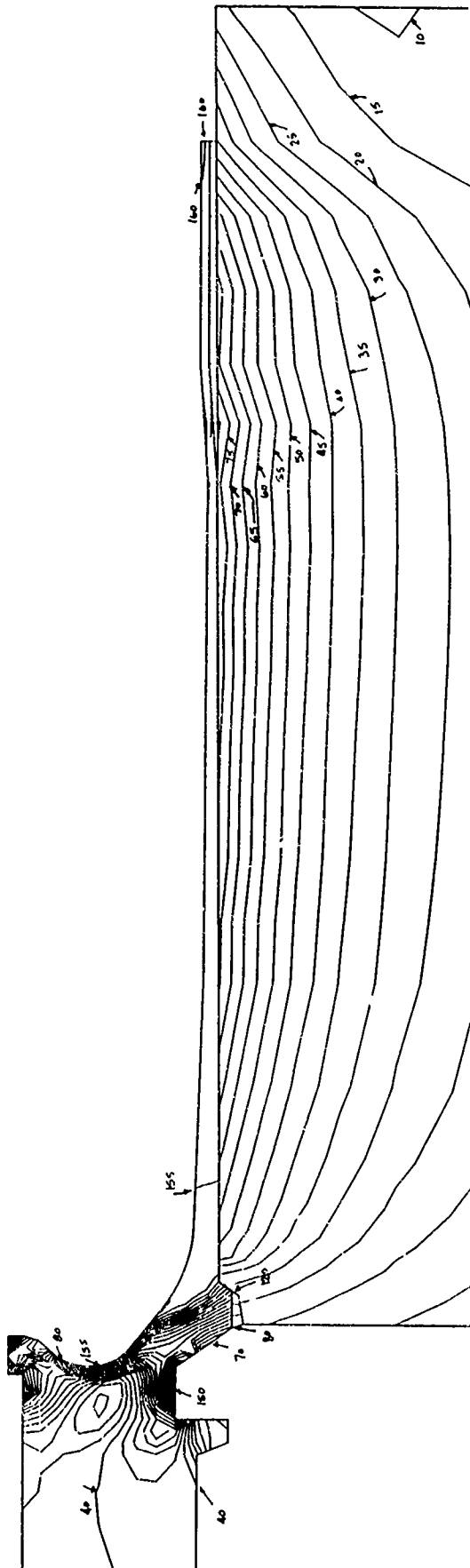
Figure 29. Equivalent stress contours, nonfrictional case, applied pressure = 40 ksi
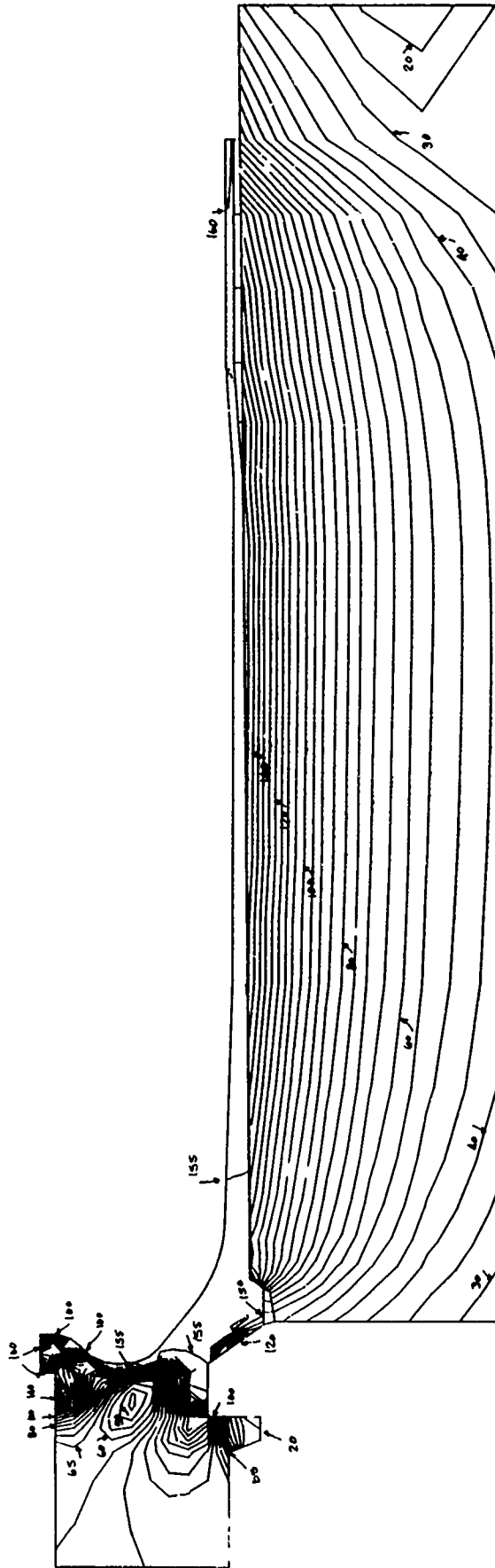
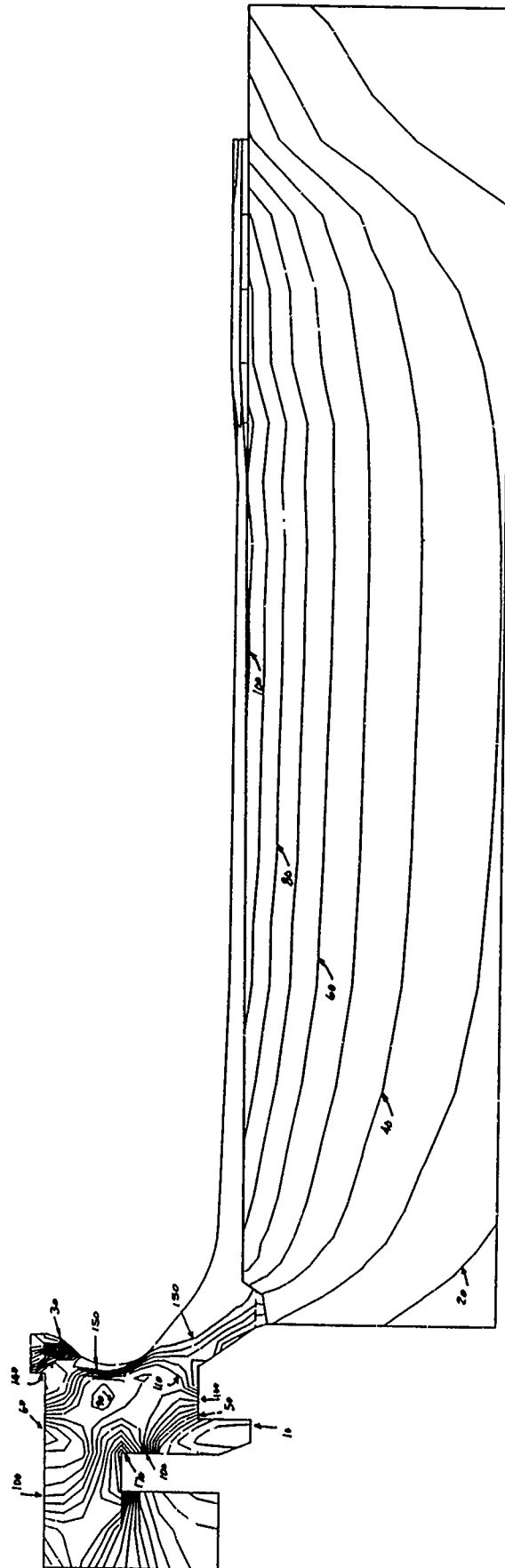Figure 30. Equivalent stress contours, nonfrictional case; applied pressure = 70 ksi

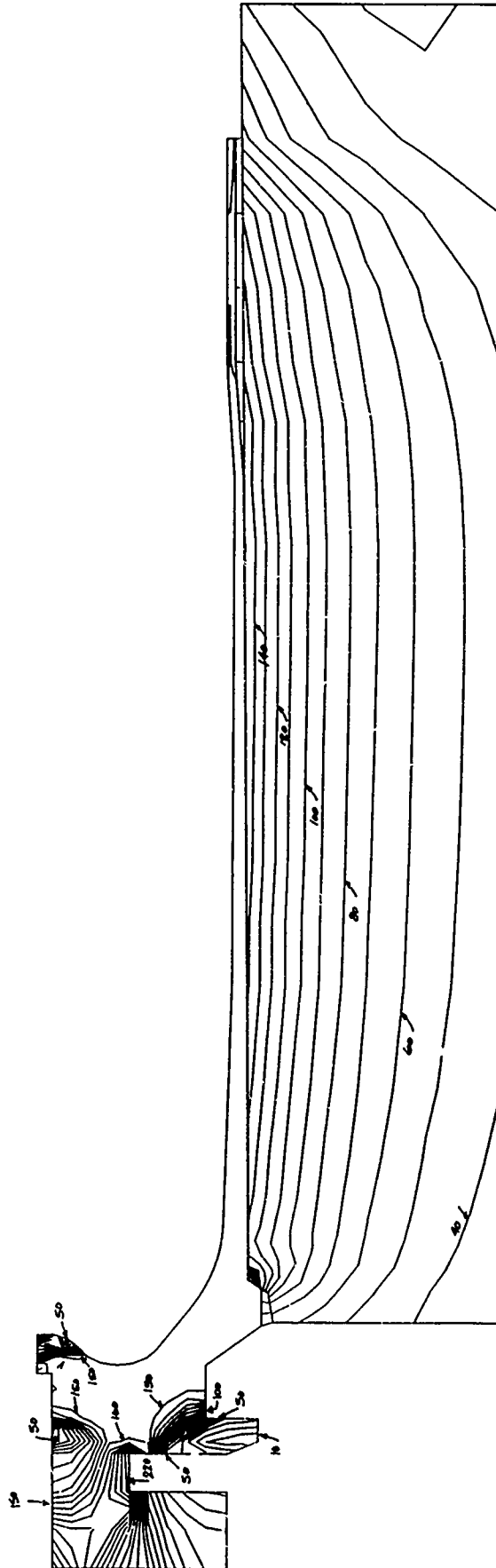Figure 31. Equivalent stress contours, minimum case-bolt contact area, applied pressure = 50 ksi

Figure 32. Equivalent stress contours, minimum case-bolt contact area, applied pressure - 70 ksi

REFERENCES

1. DeSalvo, G. and Gorman, R. W., "ANSYS Engineering System Users's Manual," Vols. I and II, Release 4.3, Swanson Analysis System, Inc., Houston, PA, June 1, 1987.

2. Nicholas, T., "Dynamic Tensile Testing of Structural Materials Using a Split Hopkinson Bar Apparatus," AFWAL-TR-80-4053, WPAFB, Ohio, October 1980.

3. Pilcher, J. O. and Wineholt, E. M., "Analysis of the Friction Behavior at High Sliding Velocities, and Pressures for Gliding Metal, Annealed Iron, Copper and Projectile Steel," Ballistic Research Laboratories, Aberdeen Proving Ground, MD, January 1977.

DISTRIBUTION LIST

Commander
Armament Research, Development and Engineering Center
U.S. Army Armament, Munitions and Chemical Command
ATTN: SMCAR-IMI-I (5)
            SMCAR-CCL-CH (4)
            SMCAR-CCL-L (2)
Picatinny Arsenal, NJ 07806-5000

Commander
U.S. Army Armament, Munitions and Chemical Command
ATTN: AMSMC-GCL(D)
Picatinny Arsenal, NJ 07806-5000

Administrator
Defense Technical Information Center
ATTN: Accessions Division (12)
Cameron Station
Alexandria, VA 22304-6145

Director
U.S. Army Materiel Systems Analysis Activity
ATTN: AMXSY-MP
Aberdeen Proving Grounds, MD 21005-5066

Commander
Chemical Research, Development and Engineering Center
U.S. Army Armament, Munitions and Chemical Command
ATTN: SMCCR-MSI
Aberdeen Proving Ground, MD 21010-5423

Commander
Chemical Research, Development and Engineering Center
U.S. Army Armament, Munitions and Chemical Command
ATTN: SMCCR-RSP-A
Aberdeen Proving Ground, MD 21010-5423

Director
Ballistic Research Laboratory
ATTN: AMXBR-OD-ST
Aberdeen Proving Ground, MD 21005-5066

Chief
Benet Weapons Laboratory, CCAC
Armament Research, Development and Engineering Center
U.S. Army Armament, Munitions and Chemical Command
ATTN: SMCAR-CCB-TL
Watervliet, NY 12189-5000

Commander
U.S. Army Armament, Munitions and Chemical Command
ATTN: SMCAR-ESP-L
Rock Island, IL 61299-6000

Director
U.S. Army TRADOC Systems Analysis Activity
ATTN: ATAA-SL
White Sands Missile Range, NM 88002